Dalton Transactions

PAPER

View Article Online
View Journal | View Issue

Cite this: *Dalton Trans.*, 2014, **43**, 8273

Reductive functionalization of a rhodium(III)–methyl bond by electronic modification of the supporting ligand†

Matthew E. O'Reilly,[a] Dale R. Pahls,[b] Joanna R. Webb,[a] Nicholas C. Boaz,[c] Subhojit Majumdar,[d] Carl D. Hoff,[d] John T. Groves,*[c] Thomas R. Cundari*[b] and T. Brent Gunnoe*[a]

Received 22nd January 2014,
Accepted 25th February 2014

DOI: 10.1039/c4dt00234b

www.rsc.org/dalton

Net reductive elimination (RE) of MeX (X = halide or pseudo-halide: Cl^-, $CF_3CO_2^-$, HSO_4^-, OH^-) is an important step during Pt-catalyzed hydrocarbon functionalization. Developing Rh(I/III)-based catalysts for alkane functionalization is an attractive alternative to Pt-based systems, but very few examples of RE of alkyl halides and/or pseudo-halides from Rh^{III} complexes have been reported. Here, we compare the influence of the ligand donor strength on the thermodynamic potentials for oxidative addition and reductive functionalization using [^{t}Bu$_3$terpy]RhCl (**1**) {^{t}Bu$_3$terpy = 4,4′,4″-tri-*tert*-butylpyridine} and [(NO$_2$)$_3$terpy]RhCl (**2**) {(NO$_2$)$_3$terpy = 4,4′,4″-trinitroterpyridine}. Complex **1** oxidatively adds MeX {X = I^-, Cl^-, $CF_3CO_2^-$ (TFA^-)} to afford [^{t}Bu$_3$terpy]RhMe(Cl)(X) {X = I^- (**3**), Cl^- (**4**), TFA^- (**5**)}. By having three electron-withdrawing NO_2 groups, complex **2** does not react with MeCl or MeTFA, but reacts with MeI to yield [(NO$_2$)$_3$terpy]RhMe(Cl)(I) (**6**). Heating **6** expels MeCl along with a small quantity of MeI. Repeating this experiment but with excess [Bu$_4$N]Cl exclusively yields MeCl, while adding [Bu$_4$N]TFA yields a mixture of MeTFA and MeCl. In contrast, **3** does not reductively eliminate MeX under similar conditions. DFT calculations successfully predict the reaction outcome by complexes **1** and **2**. Calorimetric measurements of [^{t}Bu$_3$terpy]RhI (**7**) and [^{t}Bu$_3$terpy]RhMe(I)$_2$ (**8**) were used to corroborate computational models. Finally, the mechanism of MeCl RE from **6** was investigated *via* DFT calculations, which supports a nucleophilic attack by either I^- or Cl^- on the Rh–CH_3 bond of a five-coordinate Rh complex.

Introduction

The partial oxidation of hydrocarbons into alcohols is of considerable economical interest for the production of transportation fuels and commercial chemicals.[1–4] The development of catalytic systems that can mediate an overall insertion of an oxygen-atom into a C–H bond without over-oxidation remains a substantial challenge.[4–11] Among the catalytic systems that mediate hydrocarbon functionalization,[12] Shilov's Pt-based system (Scheme 1) exerts good selectivity against over-oxidation but uses costly Pt^{IV} as the oxidant.[13] Substantial advances were made by Periana and coworkers by replacing the Pt^{IV} oxidant with H_2SO_4, but a slow turnover frequency (10^{-3} s^{-1}) and low turnover numbers caused by product inhibition and dilution with water impedes commercial application.[14] Thus, considerable research has been directed at new catalytic systems to functionalize hydrocarbons with improved

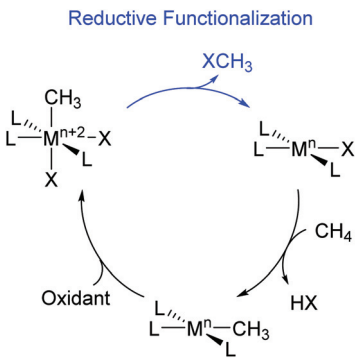

Scheme 1 The electrophilic catalytic cycle for the partial oxidation/functionalization of methane using late transition metals.

[a]*Department of Chemistry, University of Virginia, Charlottesville, Virginia 22904-4319, USA. E-mail: tbg7h@virginia.edu*
[b]*Department of Chemistry and Center for Advanced Scientific Computing and Modeling, University of North Texas, Denton, Texas 76203-5017, USA. E-mail: t@unt.edu*
[c]*Department of Chemistry, Princeton University, Princeton, New Jersey 08544, USA. E-mail: jtgroves@princeton.edu*
[d]*Department of Chemistry, University of Miami, 1301 Memorial Drive, Coral Gables, Florida 33146, USA*
† Electronic supplementary information (ESI) available: NMR spectra and experimental procedures. See DOI: 10.1039/c4dt00234b

efficiency.[12] One possible approach to improve Shilov-type chemistry is to use Rh complexes, which in general should be less electrophilic than analogous Pt complexes.

The Rh^{I}/Rh^{III} redox couple offers three attractive properties compared to Pt-based systems. (1) The less electrophilic metal should form weaker coordination bonds to water and functionalized product, potentially delaying the onset of product inhibition. (2) The easily accessible Rh^{I}/Rh^{III} redox cycle[15,16] could allow for milder and possibly air-recyclable oxidants to be used. (3) The formation of Rh(s) is less thermodynamically favorable than for Pt(s).[16,17] However, developing a Rh-based catalyst presents some challenges.[18,19]

A key step in the functionalization of hydrocarbons by Shilov-based Pt catalysts is the reductive elimination (RE) of MeX (X = halide or pseudo-halide: Cl^-, $CF_3CO_2^-$, HSO_4^-, OH^-, *etc.*) from a X–Pt(IV)–CH_3 intermediate (Scheme 1).[20,21] In fact, RE of alkyl, acyl, and aryl halides is a relatively rare transformation compared to the reverse process, oxidative addition.[22–25] The majority of examples feature high-valent late transition metal complexes: Pt(IV),[26–32] Pd^{IV},[33–38] Pd^{III},[39,40] Au^{III},[41,42] and Ni^{III} [43] complexes. RE from earlier and/or low oxidation state metals is more thermodynamically challenging. Nevertheless, Hartwig[44–46] and others[47–49] showed that RE of R–X from Pd^{II} can be achieved by employing sterically bulky phosphine ligands, and the Rh-based Monsanto acetic acid process has been shown to reversibly add $C(sp^3)$–I [50] while ultimately eliminating $C(sp^2)$–I from a Rh^{III} center prior to acetic acid formation.[51]

While the reductive functionalization from Rh^{III}–R bonds with strong phosphorus,[52,53] oxygen,[54–56] and nitrogen[54] nucleophiles has been reported, the RE of alkyl halides can be challenging. Milstein and coworkers recently reported the RE of an alkyl halide from a Rh^{III} complex using sterically bulky PCP and PNP pincer ligands to destabilize the Rh^{III}–CH_3 moiety. For these reactions, the addition of π-acidic ligands (CO, CNR, MeCN) was used to trap the Rh^{I} complex.[57,58] Steimann and coworkers reported an *in situ* Rh^{III}–CH_3 complex formed by decarbonylation, which also provides a π-acidic CO ligand to drive RE.[59]

In designing a Rh^{I}/Rh^{III} system capable of hydrocarbon functionalization, the question remains whether RE of an alkyl halide or pseudo-halide is thermodynamically feasible without significant steric destabilization. The use of large steric groups may raise the barrier for C–H activation. Hence, the thermodynamic potential for reductive functionalization should ideally be controlled by electronic modifications to the supporting ligand(s).

The terpyridine ligand provides a reasonable ligand platform to investigate the reductive functionalization from a Rh^{III}–CH_3 since the electronic properties of the terpyridine are easily modulated without appreciably impacting steric factors by appending electron-donating and withdrawing groups to the 4, 4′ and 4″ positions. The merit of using a tridentate ligand is an increased coordination stability while minimizing the electronic donation to the Rh^{III} metal center. Herein, we show that incorporating electron-withdrawing nitro groups on a terpyridine ligand sufficiently reduces the electronic stabilization of a Rh^{III}–CH_3 complex to permit reductive functionalization of MeX {X = Cl^- or $CF_3CO_2^-$ (TFA^-)}, which, to our knowledge, marks the first RE of an alkyl halide from a Rh^{III}–CH_3 without steric destabilization or the use of a trapping agent.

Results and discussion

To investigate the electronic requirements for reductive functionalization, we sought to synthesize Rh^{III}–CH_3 complexes featuring 4,4′,4″-tri-*tert*-butylterpyridine [$^tBu_3$terpy] and 4,4′,4″-trinitroterpyridine [$(NO_2)_3$terpy] ligands (eqn (1)). Incorporating *tert*-butyl groups on the terpyridine ligand enhances the solubility, while the three appended nitro groups are, on the basis of recent simulations,[60] the best suited terpyridine ligand for RE.

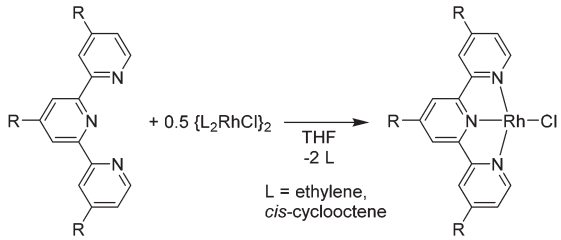

(1)

1; R = ^{t}Bu
2; R = NO_2

An easy synthetic method to access terpyridine ligated Rh^{III}–CH_3 complexes is by oxidative addition of MeI from a starting terpyridine ligated Rh^{I} complex. The synthesis of the $^tBu_3$terpy Rh^{I} complex involves combining THF solutions of $[(ethylene)_2RhCl]_2$ and $^tBu_3$terpy, which turns deep blue over 1 h yielding [$^tBu_3$terpy]RhCl (**1**) (eqn (1)). Adding hexanes to the reaction solution precipitates complex **1** as an analytically pure powder in 88% isolated yield. The nitro-substituted terpyridine complex was synthesized by a similar procedure. A THF solution of $[(COE)_2RhCl]_2$ and $(NO_2)_3$terpy was stirred overnight affording a dark blue mixture. The product [$(NO_2)_3$terpy]RhCl (**2**) (eqn (1)) was isolated as a microcrystalline powder after the addition of pentane. The poor solubility of complex **2** even in d_8-THF, CD_3NO_2, and d_6-DMSO prevents a suitable ^{1}H NMR spectrum of the complex, but combustion analysis of complex **2** provides support for the assigned molecular formula and purity.

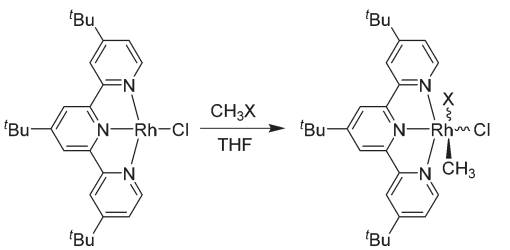

(2)

1

3; X = I
4; X = Cl
5; X = TFA

When treating complex **1** with methyl iodide in THF, the solution immediately changes color from blue to yellow-orange (eqn (2)). A small amount of yellow precipitate corresponding to a possible halide exchange product (*e.g.* (L)RhMeCl$_2$ and (L)RhMeI$_2$) was removed by filtration. Complex **3** was obtained in a 44% yield upon adding hexanes to the filtrate precipitating the desired complex as a yellow powder. The ^{1}H NMR spectrum of **3** reveals the formation of a Rh–CH$_3$ moiety appearing as a doublet at 1.13 ppm ($^2J_{Rh-H}$ = 2 Hz), and the corresponding ^{13}C nucleus resonates at 15.8 ppm ($^1J_{Rh-C}$ = 22 Hz).

Attempts at reductive functionalization involve treating complex **3** with three equivalents of [Bu$_4$N]Cl or [Bu$_4$N]TFA in CD$_3$NO$_2$. After heating at 90 °C, no functionalized product, MeCl or MeTFA, was observed. The lack of reactivity could be attributed to either a large kinetic barrier or unfavorable thermodynamics. An easier and more effective method to determine the thermodynamics of RE is to investigate the microscopic reverse reaction, oxidative addition of functionalized product MeX by **1**.

Oxidative addition of chloromethane to **1** was achieved by bubbling MeCl(g) through a THF solution of **1**. The solution changed color immediately from blue to a dark yellow. Adding hexanes to the reaction solution results in the precipitation of [^{t}Bu$_3$terpy]RhMe(Cl)$_2$ (**4**) as a yellow powder, which was isolated in 77% yield (eqn (2)). In the ^{1}H and ^{13}C{^{1}H} NMR spectra of **4**, the Rh–CH$_3$ proton and carbon atoms resonate at 0.94 ppm ($^2J_{Rh-H}$ = 2 Hz) and 5.40 ($^1J_{Rh-C}$ = 22 Hz) ppm, respectively.

Treating complex **1** with MeTFA in THF results in oxidative addition upon heating at 70 °C for 0.5 h. A substantial amount of halide exchange product precipitates from solution and was removed by filtration. Adding hexanes to the filtrate affords [^{t}Bu$_3$terpy]RhMe(Cl)(TFA) (**5**) as a pale green powder in a 41% yield (eqn (2)). The ^{1}H NMR spectrum of **5** contains a broad Rh^{III}–C*H*$_3$ resonance at 0.82 ppm, and the corresponding ^{13}C resonance appears at ~1.0 ppm. In the ^{19}F{^{1}H} NMR spectrum, the fluorine atoms resonate as a singlet at 75.4 ppm.

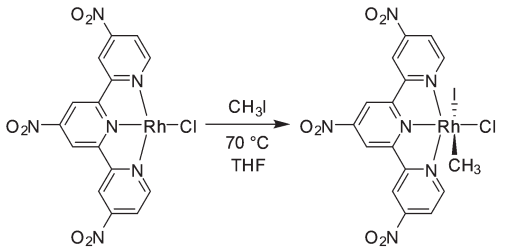

2 **6** (3)

To access a Rh^{III}–CH$_3$ complex featuring the electron-withdrawing (NO$_2$)$_3$terpy ligand, a THF suspension of complex **2** and excess MeI was heated at 70 °C for 45 minutes. A small amount of unreacted **2** remained as a solid, which was removed by filtration. Adding pentane to the reaction solution precipitates the product, [(NO$_2$)$_3$terpy]RhMe(Cl)(I) (**6**) (yield = 65%) (eqn (3)). The Rh–CH$_3$ protons resonate as a doublet at 1.05 ppm ($^2J_{Rh-H}$ = 2 Hz). The ^{13}C resonance for the methyl ligand resonates at 17.1 ppm ($^1J_{Rh-C}$ = 18 Hz), slightly downfield from complex **3**.

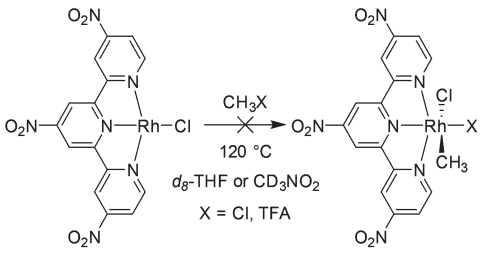

2 (4)

To test the thermodynamics for reductive functionalization of MeCl and MeTFA from complex **6**, the reverse reaction, oxidative addition, was investigated. Heating a CD$_3$NO$_2$ or d_8-THF solution containing the Rh^{I} complex **2** with excess MeCl or MeTFA at 120 °C for 18 h did not yield the oxidative addition products (eqn (4)), suggesting that reductive functionalization from the Rh^{III} complex **6** might be thermodynamically favorable.

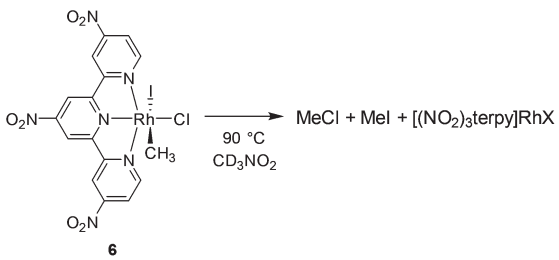

6 (5)

Heating complex **6** in d_8-THF yields an orange precipitate that still contained an intact Rh–CH$_3$ bond. However, changing the solvent to CD$_3$NO$_2$ and heating at 90 °C expels chloromethane gas (eqn (5) and Fig. 1). The quantity of MeCl(g) produced by the reaction is difficult to determine using ^{1}H NMR spectroscopy, but repeating the experiment using isotopically-labelled [(NO$_2$)$_3$terpyRh(^{13}CH$_3$)(Cl) (I) (**6***), and injecting one equivalent of MeCl gas as a standard allows a reasonable

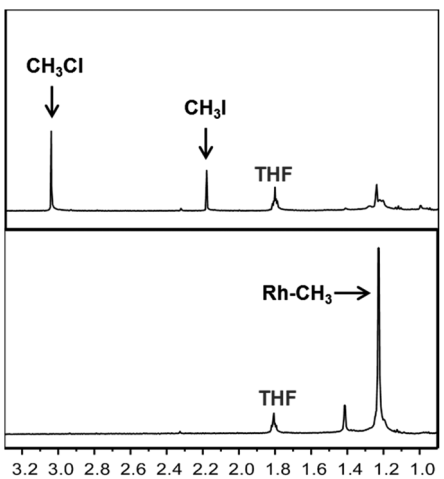

Fig. 1 Room temperature ^{1}H NMR spectra of [(NO$_2$)$_3$terpy]RhMe(Cl)(I) **6** prior to heating (bottom) and after heating at 90 °C for 10 h (top).

method to determine percent conversion based on integrated ^{13}MeCl and MeCl peaks. Overall, ^{13}MeCl forms in a ~25% yield. Methyl iodide is also observed in the reaction solution, which appears at 2.18 ppm, and constitutes a 6% conversion from the Rh–CH_3 prior to heating. Monitoring the conversion periodically by ^{1}H NMR spectroscopy, the Rh–CH_3 peak appears to slightly broaden upon heating to 90 °C. After 15 minutes, the methyl iodide peak grows in and levels off after 2 h. In contrast, the MeCl peak takes about 1 h before being sufficiently recognizable, though the accumulation of MeCl(g) may take considerable time to fill the headspace before being observed by ^{1}H NMR spectroscopy. The formation of MeCl(g) is complete after heating for 8 h. During this time, the aromatic resonances of the [$(NO_2)_3$terpy] ligand slowly disappear and a brown precipitate forms. The ^{1}H NMR spectrum of the brown precipitate in d_6-DMSO contains broad aromatic resonances arising from the terpyridine ligand, but no further identification can be made.

Considering the mixture of products, we sought to enhance the selectivity and speed of reductive functionalization by adding Cl^- to the reaction. Bercaw and coworkers reported a rate enhancement and improved selectivity for the reductive functionalization from a Pt(IV)–CH_3 complex with increasing Cl^- concentration.[20,21] We envisioned a similar effect if an S_N2 mechanism was operable for complex **6**. Treating complex **6** with three equivalents of [Bu_4N]Cl

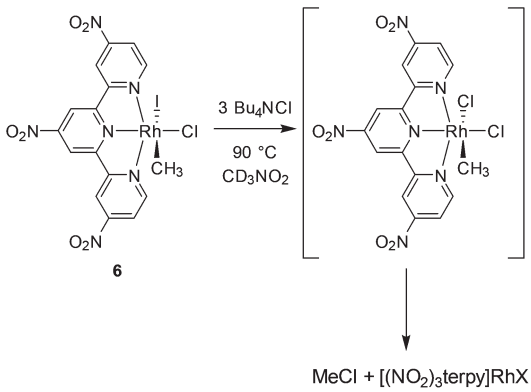

(6)

in CD_3NO_2, the Rh–CH_3 peak initially shifts from 1.04 ppm to 0.98 ppm, suggesting a halide exchange of the iodide ligand with chloride. Heating the reaction solution at 90 °C yields exclusively MeCl and Rh(I) byproduct (eqn (6)). To confirm the reductive functionalization of the Rh–CH_3 bond and quantification of MeCl, the reaction was re-attempted with **6***, which yielded $^{13}CH_3Cl$ in ~100% yield (Fig. 2). Monitoring the formation of the MeCl, the reaction appears to be complete after ~8 h, which suggests that the additional Cl^- does not provide a significant rate enhancement. Though MeI was not observed during the reaction, a notable observation is that [Bu_4N]Cl at room temperature in CD_3NO_2 can directly react with MeI to afford MeCl.

The ultimate fate of the Rh after reductive functionalization is uncertain as numerous broad aromatic resonances appear in the ^{1}H NMR spectrum. In contrast to the prior example

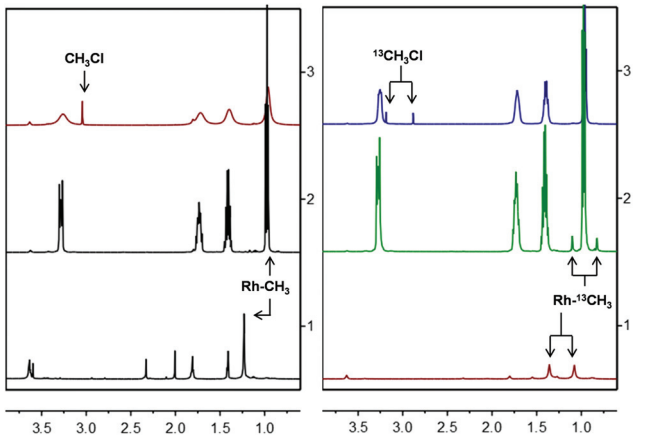

Fig. 2 RE of MeCl from **6** (left) and [$(NO_2)_3$terpy]Rh($^{13}CH_3$) (Cl)(I) **6*** (right) in CD_3NO_2. ^{1}H NMR spectra: (1) **6** and **6*** (2) with [Bu_4N]Cl, and (3) after heating at 90 °C.

where a brown precipitate forms, the reddish-brown reaction solution contains no precipitate. However, the room temperature ^{1}H NMR spectrum after reductive functionalization reveals that the Bu_4N^+ protons are significantly broadened. A possible explanation is that the tetrabutylammonium ion (a well-known phase transfer agent) assists the solvation of the Rh^I species. Verifying this hypothesis, complex **2** becomes partially soluble in CD_3NO_2 with [Bu_4N]Cl present, yielding a violet solution. Heating this purple solution at 90 °C completely dissolves the remaining solid **2** and the solution color changes from purple to reddish-brown, which is identical to the solution color after reductive functionalization. As before, the ^{1}H NMR spectrum after heating still contains multiple broad aromatic peaks, preventing further identification (see ESI†).

Without additional chloride present, we observe the formation of MeI quite readily. Thus, it was conjectured that I^- may be facilitating the RE from complex **6**, and afterwards Cl^- attacks the newly formed MeI to produce MeCl. To probe this, two equivalents of [Bu_4N]I were added to a solution of **6**. The Rh–CH_3 protons of complex **6** resonating at 1.22 ppm are unmoved by the additional I^- in solution. Heating the solution to 90 °C again releases MeCl along with MeI (6%). The typical ^{1}H NMR spectral broadening is observed upon heating to 90 °C. Monitoring the formation of MeCl, the reaction appears complete at ~2 h, though difficulty in measuring the formation of MeCl(g) and broadness of the spectrum prevent a definitive conclusion.

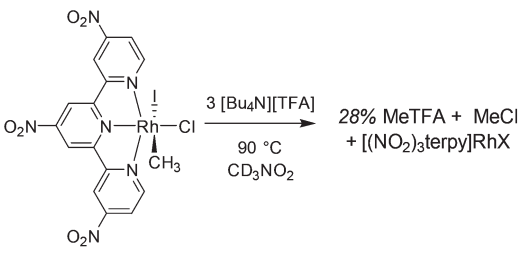

(7)

Next, we considered extending the reductive functionalization from **6** to produce MeTFA, another desirable product from electrophilic hydrocarbon functionalization. Heating a solution of **6** with three equivalents of $[Bu_4N]TFA$ yields MeTFA along with MeCl (eqn (7)). The reaction takes approximately 9 h to reach completion. The integrated ^1H (4.02 ppm) and $^{19}F\{^1H\}$ (76.7 ppm) spectra confirm a 28% conversion to MeTFA (Fig. 3). Repeating the reaction using **6*** and adding a MeCl standard, $^{13}MeCl$ produced was quantified to a ~25% yield. Again, the Bu_4N^+ protons are broad, and the Rh^I byproduct yields a reddish-brown solution that is unidentifiable by ^1H NMR spectroscopy.

Since the poor solubility of the trinitropyridine complexes prevents a full kinetic and thermodynamic investigation, DFT calculations were employed to investigate the thermodynamics and mechanism of RE from complex **6**. To best model experimental systems, structures were optimized and free energies computed in the appropriate experimental solvent using the CPCM model: THF for thermodynamics (eqn (8)) and nitromethane for mechanistic studies of reductive elimination (*vide infra*). Fig. 4 depicts the lowest energy DFT-optimized structures for complexes **1′–6′**. For simplicity, the appended ^{t}Bu groups were removed from ^{t}Bu$_3$terpy since test simulations indicate that this modification impacts absolute reaction free energies by ~0.2 kcal mol^{-1}, and relative ΔG's are expected to vary by even less (see ESI†). The optimized structures were calculated with the Rh–CH_3 bond in the axial position relative to the meridional terpyridine ligand, which is consistent with the crystallographic structures of analogous diiminepyridine Rh^{III}–CH_3 complexes.[61] In the mixed halide or pseudo-halide complexes **3′**, **5′**, and **6′**, there are two possible coordination isomers (assuming the methyl ligand remains in the axial position). Placing the more weakly coordinating iodide *trans* to the Rh–CH_3 bond lowers the energy by ~2.5 kcal mol^{-1} for **3′** and **6′**; however the two coordination isomers of **5′** are nearly thermoneutral (ΔG = 0.3 kcal mol^{-1}). The geometry of optimized structures show moderate changes in the trinitroterpyridine ligand, while the Rh–CH_3 bonds are relatively unchanged.

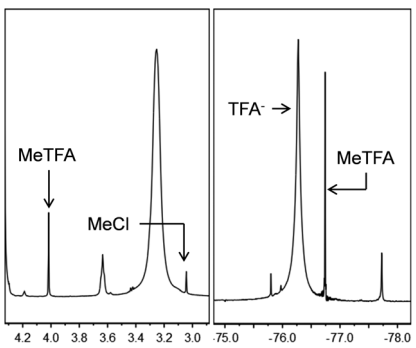

Fig. 3 Reductive elimination of MeTFA from **6**. ^1H NMR spectrum (left) and $^{19}F\{^1H\}$ NMR spectrum (right).

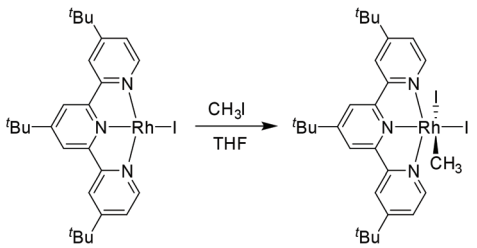

(8)

Solution calorimetric experiments were used to calibrate the computational methods. However, oxidative addition of MeX (X = I^-, Cl^-, and TFA^-) to complex **1** yields considerable amounts of halide-exchange products or uses MeCl(g), which complicates solution calorimetry experiments. To eliminate these problems, we synthesized [^{t}Bu$_3$terpy]RhI (**7**) by stirring a THF solution of **1** with excess NaI for 12 h. Treating complex **7**

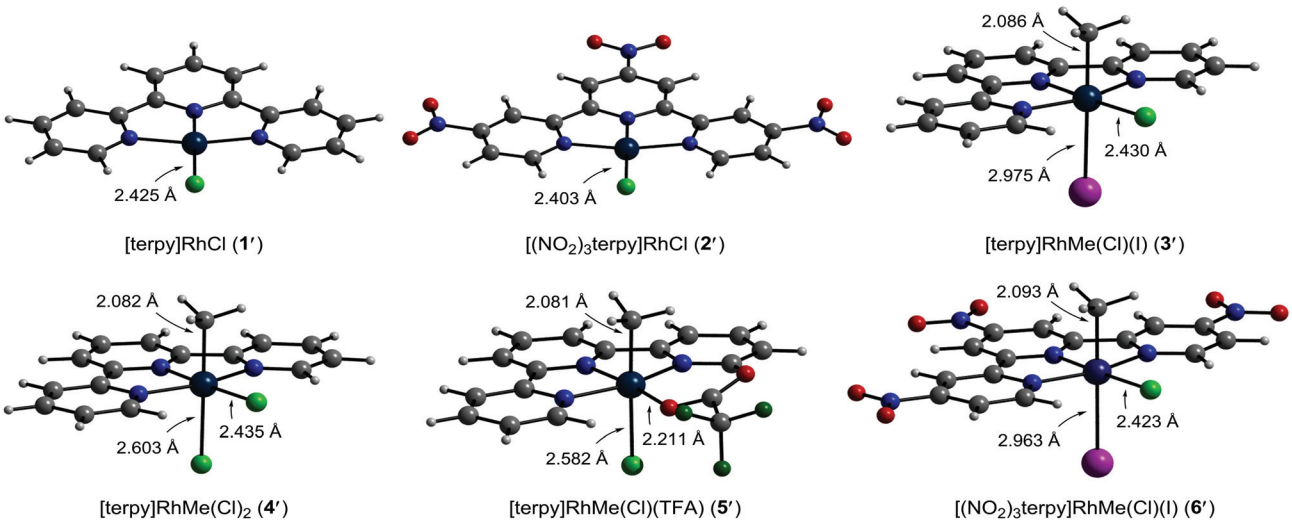

Fig. 4 DFT-optimized structures of **1′–6′** in THF. Rhodium = navy blue, carbon = gray; hydrogen = white; chlorine = lime green; iodine = purple; nitrogen = blue; oxygen = red; fluorine = forest green.

with MeI cleanly affords [^{t}Bu$_3$terpy]RhMe(I)$_2$ (**8**) (eqn (8)). Solution calorimetry experiments for the oxidative addition reaction were performed in triplicate and yielded an averaged ΔH_{rxn} of −23.5 (±0.8) kcal mol^{-1}. The corresponding reaction was modeled by DFT using [^{t}Bu$_3$terpy]RhI (**7′**) and [^{t}Bu$_3$terpy]-RhMe(I)$_2$ (**8′**); the optimized structures are presented in the ESI.† The full ligand was modeled for the calibration to minimize approximations. These parameters yielded a computed ΔH_{rxn} = −21.4 kcal mol^{-1}, which is within 2 kcal mol^{-1} of the experimental value (eqn (8)). The agreement between the experimental and theoretical thermochemistry supports the reliability of the employed computational methods.

Next, the thermodynamics of oxidative addition of MeX (X = I$^-$, Cl$^-$, TFA$^-$) to **1′** and **2′** were investigated computationally, and the results are presented in Scheme 2. The formation of **3′**, **4′**, and **5′** from **1′** was found to be exothermic by −9.4, −8.0, and −4.6 kcal mol^{-1}, respectively, while oxidative additions of MeCl and MeTFA by **2′** are uphill (1.9 and 4.9 kcal mol^{-1}). The calculations agree with the observed reactivity of complexes **1** and **2**. Perhaps more importantly, DFT calculations show a consistent ∼10 kcal mol^{-1} difference for the oxidative addition reactions between complexes **1′** and **2′**, illustrating the substantial influence of the NO_2 groups on the free energy potentials. A surprising result is that the calculated free energy for the oxidative addition of MeI by **2′** to give **6′** is 0.8 kcal mol^{-1} uphill. Taking into account that our computational model underestimates the ΔH_{rxn} by about 2 kcal mol^{-1}, the mild free energy difference corresponding to a K_{eq} = 0.16 {K_{eq} = [**6′**]/([**2′**][MeI])} suggests a near thermoneutral reaction. Experimental evidence seems to support this assertion, though the reaction conditions are complicated due to solubility, side-reactions, and temperature. Nevertheless, the 10-fold excess of MeI in THF at 70 °C may drive the reaction towards the formation of **6** (isolated yield = 44%), while in the absence of MeI, complex **6** was shown to reductively eliminate a small percentage of MeI along with MeCl in CD_3NO_2 at 90 °C.

The mechanism of RE, the microscopic reverse of oxidative addition, has been proposed to occur by either concerted RE, S_N2, or radical pathways.[51] Often more than one mechanism may be operable depending on the nature of X$^-$.[57,62] More electron donating X$^-$ favor concerted RE mechanism over an S_N2 pathway. For instance, Milstein and coworkers propose a concerted RE of MeCl(*g*) while an S_N2 RE pathway was operative for MeBr and MeI.[57]

In our case, we sought to investigate the mechanism of reductive functionalization of MeCl from complex **6′** with free Cl$^-$ present in solution for two reasons. First, the RE of MeCl from **6** with three equivalents of [Bu$_4$N]Cl exclusively yields MeCl, and secondly, NMR data indicate that the coordinated iodide is substituted with chloride upon adding [Bu$_4$N]Cl, providing [(NO$_2$)$_3$terpy]RhMe(Cl)$_2$ (**9′**) as a reasonable starting position. We calculated three pathways (Fig. 5), and for each pathway we modeled six-coordinate and five-coordinate Rh (formed by dissociation of Cl$^-$ from **9′**) transition states. Here, we present results supporting an S_N2 RE mechanism through a five-coordinate [(NO$_2$)$_3$terpy]RhMe(Cl)$^+$ (**11′**) intermediate.

To keep the calculations consistent with the experimental work, we employed the same level of theory used in our previous calibration study, but changed the continuum solvent to CH_3NO_2. In this solvent, the RE of MeCl from **9′** is calculated to be modestly favorable (−0.3 kcal mol^{-1}). Fig. 5 depicts three different plausible mechanisms for RE labeled as Pathways A, B, and C. We excluded a radical mechanism since CD_3NO_2 is a known radical trap.[63–65] To simplify matters, complete separation of ions was assumed, so no tetrabutyl ammonium cations were modeled as spectator cations. All isolated anions were modeled in continuum CH_3NO_2 solvent to balance equations.

Pathway A features a concerted RE of MeCl. The calculated free energy barrier from **9′** (**TS-A1**) is 49.7 kcal mol^{-1}. One approach to mitigate the high transition state barrier is to remove *trans*-Cl$^-$ (forming **11′**) prior to the reductive functionalization step. Previous RE studies reveal that odd-coordinate complexes yield overall lower energy pathways for RE.[20,21,27,28,57,58,66] The initial loss of chloride ion from **9′** yielding **11′** is mildly endergonic (7.8 kcal mol^{-1}), but lowers

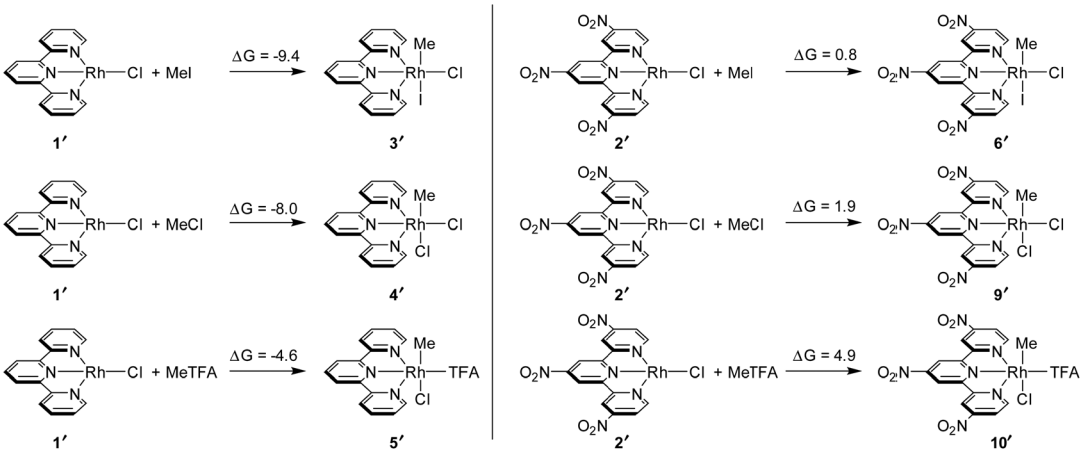

Scheme 2 DFT calculated thermodynamics for the reaction of **1′** and **2′** with MeX. All free energies (kcal mol^{-1}) are listed as L_nRh^{I} + MeX → L_nRh^{III}. Numerical values are calculated thermodynamics in continuum THF solvent.

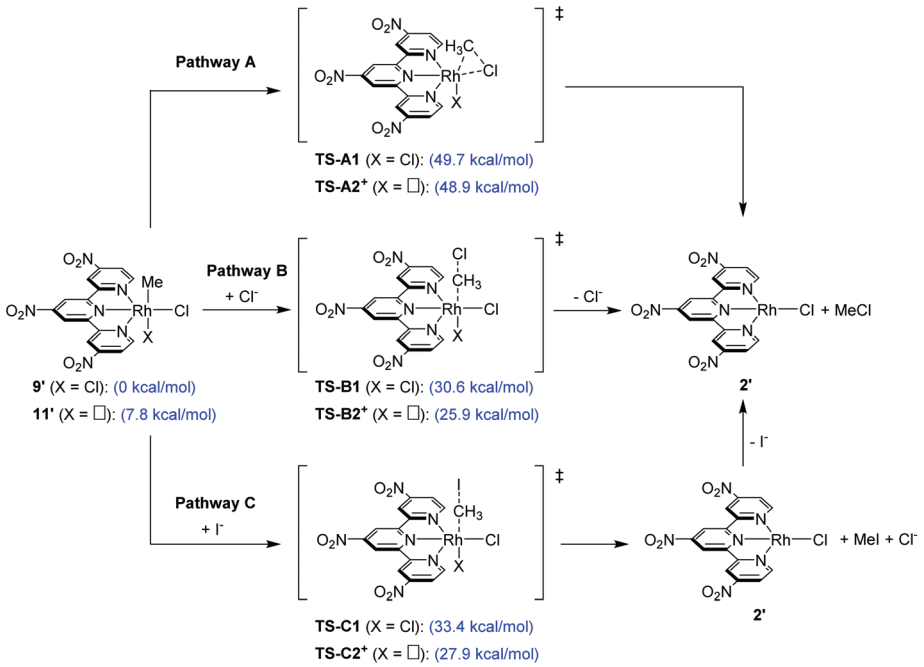

Fig. 5 Three pathways for reductive functionalization from **9′**. Pathway A: Concerted RE, pathway B: Cl^- initiated S_N2 RE, and pathway C: I^- initiated S_N2 RE. Numerical values are calculated free energies (kcal mol^{-1}) in continuum CH_3NO_2 solvent relative to **9′**. **TS-1** involve six-coordinate Rh transition states, **TS-2** involve five-coordinate Rh transition states (square denotes a vacant coordination site).

the overall TS barrier by 0.8 kcal mol^{-1} (**TS-A2**$^+$, 48.9 kcal mol^{-1}). Regardless, both transition states are exceptionally high for a reaction that proceeds at 90 °C.

Pathways B and C (Fig. 5) involve a nucleophilic attack upon the Rh–Me bond by free Cl^- or I^-, respectively. This mechanism – an S_N2 mechanism – parallels organic substitution reactions. A nucleophilic attack by the chloride (Pathway B) directly on **9′** (**TS-B1**) gives a barrier of 30.6 kcal mol^{-1}. By removing the *trans*-chloride ligand prior to reductive functionalization, the transition state barrier (**TS-B2**$^+$) is lowered by 4.7 kcal mol^{-1}, yielding the lowest computed free energy barrier of 25.9 kcal mol^{-1} (relative to **9′**). This energetic barrier appears reasonable in relation to the required reaction conditions. The other possible pathway for reductive functionalization (Pathway C) is a nucleophilic attack by I^-, which is also present in solution. Iodide serves an intermediary role by forming MeI, which would then react with free Cl^- to generate MeCl. The calculated transition state barrier for iodide attack on complexes **9′** and **11′** yielded slightly higher free energies, 33.4 and 27.9 kcal mol^{-1}, respectively, than for Pathway B (Fig. 5).

The DFT calculations provide three insights into the mechanism of reductive functionalization from **9′** (Fig. 6). (1) An S_N2 pathway is heavily favored over a concerted RE mechanism. (2) Dissociating the *trans*-halide to form cationic complex **11′** prior to reductive functionalization lowers the transition state barrier to nucleophilic attack by ~5 kcal mol^{-1}. (3) While Pathway B yields the lowest transition state barrier, it is possible that Pathway C is also operable since the calculations reveal only a slight 2 kcal mol^{-1} difference for chloride

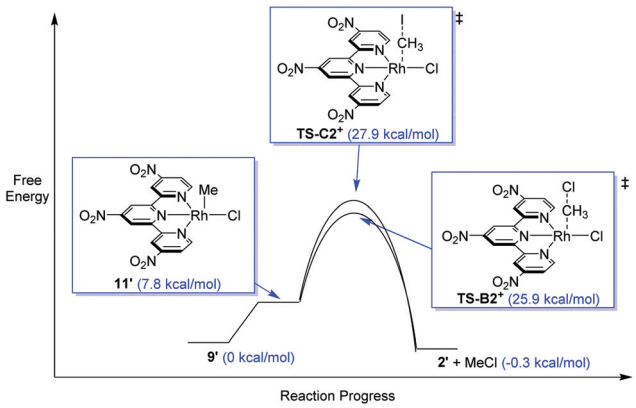

Fig. 6 Free energy diagram depicting the two viable pathways the reductive functionalization of Rh–CH_3 bond from **9′** through **11′**.

(**TS-B2**$^+$) *versus* iodide (**TS-C2**$^+$) attack on **11′**. Though caution should be exercised due to the known uncertainties in DFT transition state energies, some experimental evidence may support this ordering. RE from **6** in the absence of $[Bu_4N]Cl$ yields MeI alongside MeCl. This evidence strongly supports that Pathway C as an additional operable mechanism.

Conclusions

Reported herein is the synthesis of Rh(I) complexes **1** and **2** featuring two different electronic environments. For complex **1**, the Rh(I) metal center is situated within the strongly

reducing environment of the $^{t}Bu_3$terpy ligand and readily activates MeX (X = I^-, Cl^-, TFA^-) to afford Rh^{III}–CH_3 complexes **3**, **4**, and **5**, respectively. By replacing the three *t*-butyl substituents with three nitro groups, the ligand's donating ability is drastically diminished, which reduces the metal's potential in complex **2** towards oxidative addition. Evidence is that complex **2** is unreactive towards MeCl or MeTFA. DFT calculations predict the direction of oxidative addition and reductive functionalization by complexes **1** and **2**. Furthermore, solution calorimetry experiments for oxidative addition of MeI by **7** to form **8** closely matched calculated ΔH_{rxn}, bolstering confidence in our computational methods.

Oxidative addition of MeI by **2** provides access to a trinitroterpyridine ligated Rh^{III}–CH_3 complex **6** in order to investigate reductive functionalization. Heating complex **6** in CD_3NO_2 reductively eliminates MeCl along with MeI. Upon addition of free Cl^- and TFA^- complex **2** undergoes reductive functionalization to produce MeCl and MeTFA, respectively. DFT calculations support an S_N2 reductive functionalization pathway through a five-coordinate intermediate $[(NO_2)_3terpy]RhMe(Cl)^+$ (**11′**). The slight energetic difference between transition state for Cl^- and I^- attack on **11′** suggests that both routes are competitive.

Net reductive elimination of RX is a key step in overall catalytic cycles for hydrocarbon functionalization. Thus, a primary limitation to use of Rh complexes as catalysts for hydrocarbon functionalization through the "Shilov" route (Scheme 1) is the energetic inhibition (both kinetic and thermodynamic) of RX elimination. For the first time, we are able to establish that the RE of an alkyl halide (MeCl) and pseudo-halide (MeTFA) from a Rh^{III} complex can be achieved without using sterically bulky ligands or a trapping agent to stabilize the Rh(I) product. These results are promising for Rh-based electrophilic catalysts for hydrocarbon functionalization. Ongoing work focuses on developing new systems capable of both RE and C–H bond activation, and progressing towards the conditions needed for catalytic hydrocarbon functionalization.

Acknowledgements

The authors (MEO, DRP, JRW, NCB, JTG, TRC, TBG) acknowledge support from the Center for Catalytic Hydrocarbon Functionalization, an Energy Frontier Research Center funded by the US Department of Energy, Office of Science, Office of Basic Energy Sciences under Award Number DESC0001298 as well as (SM, CDH) the Petroleum Research Fund administered by the American Chemical Society 51756-ND3.

Notes and references

1 G. A. Olah and Á. Molnár, *Hydrocarbon chemistry*, John Wiley, Hoboken, N.J., 2nd edn, 2003.
2 H. Wittcoff, B. G. Reuben and J. S. Plotkin, *Knovel Biochemistry Biology & Biotechnology Library – Academic Collection; Knovel Chemistry & Chemical Engineering Library – Academic Collection*, Wiley-Interscience, Hoboken, N.J., 2nd edn, 2004.
3 W. B. Tolman, *Activation of small molecules: organometallic and bioinorganic perspectives*, Wiley-VCH, Weinheim, 2006.
4 J. A. Labinger, *J. Mol. Catal. A: Chem.*, 2004, **220**, 27.
5 B. L. Conley, W. J. Tenn, K. J. H. Young, S. K. Ganesh, S. K. Meier, V. R. Ziatdinov, O. Mironov, J. Oxgaard, J. Gonzales, W. A. Goddard and R. A. Periana, *J. Mol. Catal. A: Chem.*, 2006, **251**, 8.
6 R. H. Crabtree, *J. Chem. Soc., Dalton Trans.*, 2001, 2951.
7 K. I. Goldberg and A. S. Goldman, *Activation and functionalization of C-H bonds*, American Chemical Society, Division of Inorganic Chemistry; Distributed by Oxford University Press, Washington, DC, 2004.
8 J. A. Labinger and J. E. Bercaw, *Nature*, 2002, **417**, 507.
9 R. A. Periana, G. Bhalla, W. J. Tenn, K. J. H. Young, X. Y. Liu, O. Mironov, C. J. Jones and V. R. Ziatdinov, *J. Mol. Catal. A: Chem.*, 2004, **220**, 7.
10 J. R. Webb, T. Bolano and T. B. Gunnoe, *ChemSusChem*, 2011, **4**, 37.
11 E. G. Chepaikin, *Russ. Chem. Rev.*, 2011, **80**, 363.
12 B. G. Hashiguchi, S. M. Bischof, M. M. Konnick and R. A. Periana, *Acc. Chem. Res.*, 2012, **45**, 885.
13 N. F. Goldshledger, A. A. Shteinman, A. E. Shilov and V. V. Eskova, *Russ. J. Phys. Chem.*, 1972, **46**, 785.
14 R. A. Periana, D. J. Taube, S. Gamble, H. Taube, T. Satoh and H. Fujii, *Science*, 1998, **280**, 560.
15 $Rh^+ \rightarrow Rh^{3+} + 2e^-$; $E^\circ = -0.158$ V *vs.* $PtCl_4^{2-} + 2Cl^- \rightarrow PtCl_6^{2-} + 2e^-$; $E^\circ = -0.68$ V.
16 Chemical Rubber Company, CRC Press, Cleveland, Ohio, 1978.
17 $Rh^+ + e^- \rightarrow Rh$; $E^\circ = 0.6$ V *vs.* $Pt^{2+} + 2e^- \rightarrow Pt$; $E^\circ = 1.18$ V.
18 K. A. Manbeck, W. W. Brennessel and W. D. Jones, *Inorg. Chim. Acta*, 2013, **397**, 140.
19 J. Kovach, W. W. Brennessel and W. D. Jones, *Inorg. Chim. Acta*, 2011, **367**, 108.
20 G. A. Luinstra, L. Wang, S. S. Stahl, J. A. Labinger and J. E. Bercaw, *J. Organomet. Chem.*, 1995, **504**, 75.
21 G. A. Luinstra, J. A. Labinger and J. E. Bercaw, *J. Am. Chem. Soc.*, 1993, **115**, 3004.
22 J. D. Atwood, *Inorganic and organometallic reaction mechanisms*, Wiley-VCH, New York, 2nd edn, 1997.
23 R. H. Crabtree, *The organometallic chemistry of the transition metals*, Wiley-Interscience, Hoboken, N.J., 4th edn, 2005.
24 A. Vigalok, *Chem. - Eur. J.*, 2008, **14**, 5102.
25 A. Vigalok and A. W. Kaspi, *Top. Organomet. Chem.*, 2010, **31**, 19.
26 R. Ettorre, *Inorg. Nucl. Chem. Lett.*, 1969, **5**, 45.
27 K. I. Goldberg, J. Y. Yan and E. M. Breitung, *J. Am. Chem. Soc.*, 1995, **117**, 6889.
28 K. I. Goldberg, J. Y. Yan and E. L. Winter, *J. Am. Chem. Soc.*, 1994, **116**, 1573.
29 J. D. Ruddick and B. L. Shaw, *J. Chem. Soc. A*, 1969, 2969.
30 A. Yahav-Levi, I. Goldberg and A. Vigalok, *J. Am. Chem. Soc.*, 2006, **128**, 8710.

31 A. Yahav-Levi, I. Goldberg, A. Vigalok and A. N. Vedernikov, *J. Am. Chem. Soc.*, 2008, **130**, 724.
32 A. Yahav-Levi, I. Goldberg, A. Vigalok and A. N. Vedernikov, *Chem. Commun.*, 2010, **46**, 3324.
33 P. L. Arnold, M. S. Sanford and S. M. Pearson, *J. Am. Chem. Soc.*, 2009, **131**, 13912.
34 T. Furuya and T. Ritter, *J. Am. Chem. Soc.*, 2008, **130**, 12834.
35 A. W. Kaspi, A. Yahav-Levi, I. Goldberg and A. Vigalok, *Inorg. Chem.*, 2008, **47**, 5.
36 K. B. McMurtrey, J. M. Racowski and M. S. Sanford, *Org. Lett.*, 2012, **14**, 4094.
37 J. M. Racowski, J. B. Gary and M. S. Sanford, *Angew. Chem., Int. Ed.*, 2012, **51**, 3414.
38 S. R. Whitfield and M. S. Sanford, *J. Am. Chem. Soc.*, 2007, **129**, 15142.
39 D. C. Powers, D. Benitez, E. Tkatchouk, W. A. Goddard and T. Ritter, *J. Am. Chem. Soc.*, 2010, **132**, 14092.
40 X. Q. Shen, A. M. Hyde and S. L. Buchwald, *J. Am. Chem. Soc.*, 2010, **132**, 14076.
41 N. P. Mankad and F. D. Toste, *Chem. Sci.*, 2012, **3**, 72.
42 V. J. Scott, J. A. Labinger and J. E. Bercaw, *Organometallics*, 2010, **29**, 4090.
43 A. T. Higgs, P. J. Zinn, S. J. Simmons and M. S. Sanford, *Organometallics*, 2009, **28**, 6142.
44 A. H. Roy and J. F. Hartwig, *J. Am. Chem. Soc.*, 2001, **123**, 1232.
45 A. H. Roy and J. F. Hartwig, *J. Am. Chem. Soc.*, 2003, **125**, 13944.
46 A. H. Roy and J. F. Hartwig, *Organometallics*, 2004, **23**, 1533.
47 H. Liu, C. L. Li, D. Qiu and X. F. Tong, *J. Am. Chem. Soc.*, 2011, **133**, 6187.
48 J. Pan, X. Y. Wang, Y. Zhang and S. L. Buchwald, *Org. Lett.*, 2011, **13**, 4974.
49 D. A. Petrone, H. A. Malik, A. Clemenceau and M. Lautens, *Org. Lett.*, 2012, **14**, 4806.
50 P. M. Maitlis, A. Haynes, G. J. Sunley and M. J. Howard, *J. Chem. Soc., Dalton Trans.*, 1996, 2187.
51 J. F. Hartwig, *Organotransition metal chemistry: from bonding to catalysis*, University Science Books, Sausalito, California, 2010.
52 A. P. Nelson and S. G. DiMagno, *J. Am. Chem. Soc.*, 2000, **122**, 8569.
53 E. P. Shestakova, Y. S. Varshavsky and A. B. Nikolskii, *J. Organomet. Chem.*, 2005, **690**, 3397.
54 M. S. Sanford and J. T. Groves, *Angew. Chem., Int. Ed.*, 2004, **43**, 588.
55 B. Wu, J. D. Zhang, L. Yun and X. F. Fu, *Dalton Trans.*, 2011, **40**, 2213.
56 H.-Z. Han, Ph.D. Thesis, Princeton University, 1992.
57 M. Feller, Y. Diskin-Posner, G. Leitus, L. J. W. Shimon and D. Milstein, *J. Am. Chem. Soc.*, 2013, **135**, 11040.
58 C. M. Frech and D. Milstein, *J. Am. Chem. Soc.*, 2006, **128**, 12434.
59 E. Lindner, Q. Y. Wang, H. A. Mayer, R. Fawzi and M. Steimann, *Organometallics*, 1993, **12**, 1865.
60 D. R. Pahls, J. T. Groves, T. B. Gunnoe and T. R. Cundari, DOI: 10.1021/om4010093.
61 H. F. Haarman, J. M. Ernsting, M. Kranenburg, H. Kooijman, N. Veldman, A. L. Spek, P. W. N. M. van Leeuwen and K. Vrieze, *Organometallics*, 1997, **16**, 887.
62 J. A. Labinger, J. A. Osborn and N. J. Coville, *Inorg. Chem.*, 1980, **19**, 3236.
63 D. Behar and R. W. Fessende, *J. Phys. Chem.*, 1972, **76**, 1710.
64 B. C. Gilbert, J. P. Larkin and R. O. C. Norman, *J. Chem. Soc., Perkin Trans. 2*, 1972, 1272.
65 K. J. Reszka, P. Bilski, C. F. Chignell and J. Dillon, *Free Radical Biol. Med.*, 1996, **20**, 23.
66 M. Feller, M. A. Iron, L. J. W. Shimon, Y. Diskin-Posner, G. Leitus and D. Milstein, *J. Am. Chem. Soc.*, 2008, **130**, 14374.